

LNAPL INFILTRATION AND DISTRIBUTION IN UNSATURATED POROUS MEDIA - IMPLEMENTATION OF IMAGE ANALYSIS TECHNIQUE

F. SIMANTRAKI, M. AIVALIOTI, E. GIDARAKOS

Laboratory of Toxic and Hazardous Waste Management, Department of Environmental Engineering, Technical University of Crete, University Campus, 73100, Chania, Greece

SUMMARY: Light non-aqueous phase liquids (LNAPL) represent a great category of soil contaminants that can consist a persistent, secondary and long term source of contamination. In order to successfully confront with LNAPL pollution, their infiltration and distribution in the subsurface must be studied. The purpose of this project was to investigate the flow and distribution of two typical LNAPL (Soltrol 220 and Diesel Fuel) in two different types of unsaturated porous media (sands). Four LNAPL spills were simulated in an experimental sand matrix and images were taken under stable conditions. Two types of sand configurations were studied, specifically, two experiments consisted of LNAPL infiltration into a coarse sand layer upper a fine sand layer whereas the last two experiments had the inverse sand configuration. The movement of the liquid was defined by an image analysis technique and finally saturation profiles were produced, allowing the study of LNAPL infiltration and distribution. As it was expected, LNAPL moved slower in the fine sand than in the coarse sand, due to its small coefficient of permeability. LNAPL saturation was estimated to be 80-100% mainly in the interface of the two sand layers, where vertical movement was limited and horizontal dominated. It was proved that the interface of fine and coarse layer is able to act as a capillary barrier which prevents the LNAPL infiltration in the coarse layer.

1. INTRODUCTION

Light Non-Aqueous Phase Liquids (LNAPL) are immiscible, have low water solubility and, in the case of a spill on the soil surface, tend to stay entrapped in the vadose zone of the subsurface, causing residual contamination. In most cases, they become persistent sources of contamination that can greatly influence the quality of the underlying aquifer. While knowledge of LNAPL distribution in the subsurface is important, in order to implement effective remediation measures at contaminated sites, the complexity of LNAPL flow is little understood, since it is determined by a complex interaction between gravity and viscous capillary forces. Therefore several

experimental studies have been conducted on LNAPL distribution within the soil, e.g. (Van Geel et al. 1994, Wipfler et al 1999).

The objective of this paper is to present data sets which result from two-dimensional flow experiments that simulate the spill of two typical LNAPL in an unsaturated porous medium (sand). For this purpose a special MatLab algorithm was developed and applied. This algorithm allowed a detailed qualitative mapping of the LNAPL infiltration and distribution, as well as a profile of the LNAPL saturation throughout the plume area. The results of this study can be further used to validate existing numerical models and simulate real field conditions.

2. EXPERIMENTAL MATERIALS AND METHODS

2.1 Experimental apparatus and procedure

For the laboratory simulation of a LNAPL spill a rectangular cell of 100cm in length, 120 cm in height and 2 cm in depth was made out of glass. The glass cell was filled with deionized water and sand was dropped in, using a sand pouring apparatus, until a sand matrix of 44cm height was achieved. After the packing, water was removed through two valves at the bottom of the cell and sand was allowed to dry for several days at room temperature. Afterwards, 100 ml of LNAPL were added on the surface of the sand matrix dropwise at a rate of 1 ml/min, using a peristaltic pump. LNAPL was colored with 0,003% Sudan III. The whole matrix was photographed at regular time intervals, in order to depict the LNAPL movement versus time.

Four experiments were conducted, using, respectively:

- Soltrol 220 and a series of coarse sand layer (12 cm height) and fine sand layer (35 cm height).
- Diesel Fuel and a series of coarse sand layer (10 cm height) and fine sand layer (34 cm height).
- Soltrol 220 and a series of fine sand layer (4 cm height) and coarse sand layer (4 cm height).
- Diesel Fuel and a series of fine sand layer (4 cm height) and coarse sand layer (4 cm height).

Capillary pressure measurements were conducted via a tensiometer (SKTD 690) which was buried in sand with known saturation in order to create the *k-s-p* curves that correspond to each one of our experiments.

2.2 Porous medium and LNAPL properties

The basic particle size distribution parameters of the two types of sand used for the flow experiments are shown in Table 1.

Table 1.. Typical particle size distribution parameters of the sands used.

Sand Type	Medium grain size (mm)		Uniformity coefficient Cu (d ₆₀ /d ₁₀)
	d ₁₀	d ₆₀	
Fine	0.09	0.5	5.6
Coarse	0.18	1.98	11

As far as the hydraulic properties of the sands are concerned, flow rate experiments using water provided the following values of coefficient of permeability (*k*): $8.53 \cdot 10^{-6}$ cm/s for the fine sand and $1.5 \cdot 10^{-5}$ cm/s for the coarse sand. Based on these values, the desired absolute permeability *K*

was estimated based on the following equation: $k = \frac{K \rho g}{\mu} \rightarrow K = \frac{k \mu}{\rho g}$

where *K* is the absolute permeability (m²), ρ is the fluid density (kg/cm³), *g* is the gravity

acceleration constant (cm/s^2) and μ is the fluid viscosity (kg/cm s).

Finally, both sands porosity n was calculated using the Karman-Cozeny equation (I lead, 1992):

$$k = \frac{\rho \cdot g}{C \cdot f \cdot \mu \cdot S^2} \cdot \frac{e^3}{1-e}$$

where C is a shape factor, equal to 5 for spherical particles, f is an angularity factor, S is the specific surface of sand grain (mm^{-1}) and e is a parameter related to porosity, as follows:

$$n = \frac{e}{1-e}$$

Table 2 presents the results of the above described calculations.

Table 2. Hydraulic properties of the sands used.

Parameter	Porosity n	Absolute permeability K_{diesel} (m^2)	Absolute permeability K_{soltrol} (m^2)
Fine sand	0.37	$3.66 \cdot 10^{-13}$	$3.23 \cdot 10^{-13}$
Coarse sand	0.42	$6.43 \cdot 10^{-12}$	$5.69 \cdot 10^{-12}$

The first LNAPI, used was Soltrol 220 (Cevron Phillips Chemical Company, USA). Soltrol 220 is an isoparaffinic solvent, mixture of C13 to C17 hydrocarbons chains. It has negligible solubility in water, low vapor pressure (27.6 Pa), gravity density of 0.79 g/cm^3 and viscosity of 0.0048 Pa s . The interfacial tensions between Soltrol 220 - water and Soltrol 220 - air are 0.036 and 0.026 N/m , respectively (Kechavarzi et al. 2005). Soltrol is colorless; so in order to enhance visual observations and achieve optimum results using image analysis technique, it was dyed red using 0.003% Sudan III.

The second LNAPI, used was Diesel fuel (Hellenic Petroleum S.A., Greece). Diesel has negligible solubility in water, low vapor pressure (27.6 Pa), gravity density of 0.84 g/cm^3 and viscosity of 0.0036 Pa s . The interfacial tension between Diesel - air is 0.05 N/m . Diesel is also almost colorless and it therefore was dyed red using 0.003% Sudan III.

3. IMAGE ANALYSIS TECHNIQUE

3.1 General

Color can be expressed in different formats. Perhaps the most common one is as a combination of red, green and blue (RGB); a format used by video cameras and computer graphics. Hue, Saturation and Intensity (HSI) are vector components of another format, which is used for color specification. In HSI format, hue is the color attribute that describes the pure color, saturation corresponds to the degree to which the color is diluted with white and intensity corresponds to the grey level.

In order to convert RGB into HSI, hue can be expressed as (Wilson 1988):

$$H = 225 \left\{ \frac{1}{360} \left[Y - \arctan \frac{2R - G - B}{\sqrt{3}(G - B)} \right] \right\}$$

Intensity (I) is calculated as [Darnault et al. 1997]: $I = 255 \left(\frac{R+G+B}{3} \right)$

3.1 Calibration of the method

In order to define LNAPL saturation during the experiment, a calibration scale was created for both sands and LNAPL. The calibration cells were filled with the same coarse and fine sand that was used for the flow experiments. Certain volume of LNAPL was added in the cells, so as to achieve 0, 20, 40, 60, 80, 100 % of LNAPL saturation. Images of the calibration cells were taken under constant lighting conditions. These images were edited using a MatLab algorithm that estimates the average intensity for every image. As a result, every LNAPL saturation percentage corresponds to a certain value of mean intensity. Table 3 contains the calibration data for the coarse and fine sand for both LNAPL. These values were used to create a calibration scale, on which the definition of LNAPL saturation in every pixel of the images was based.

Table 3. Calibration data for the coarse and fine sand.

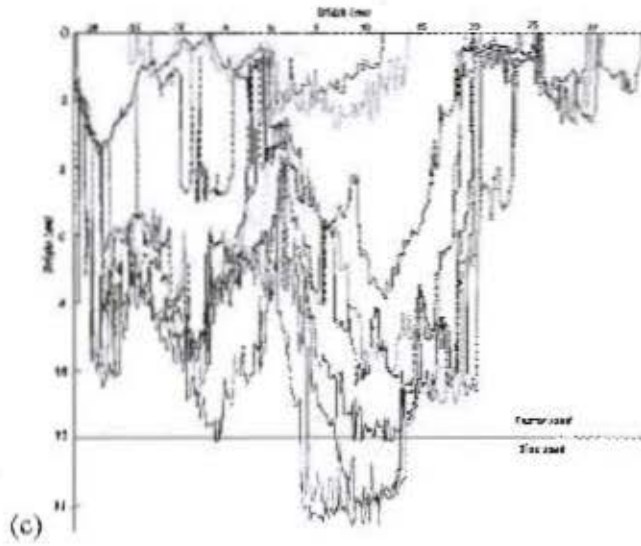
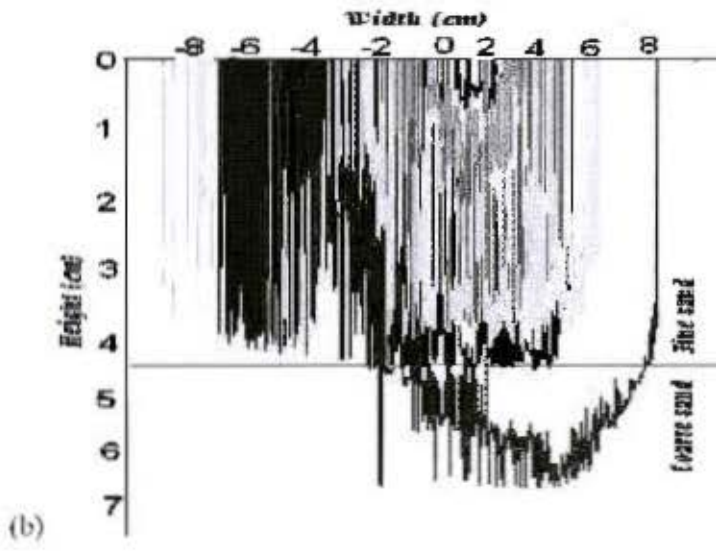
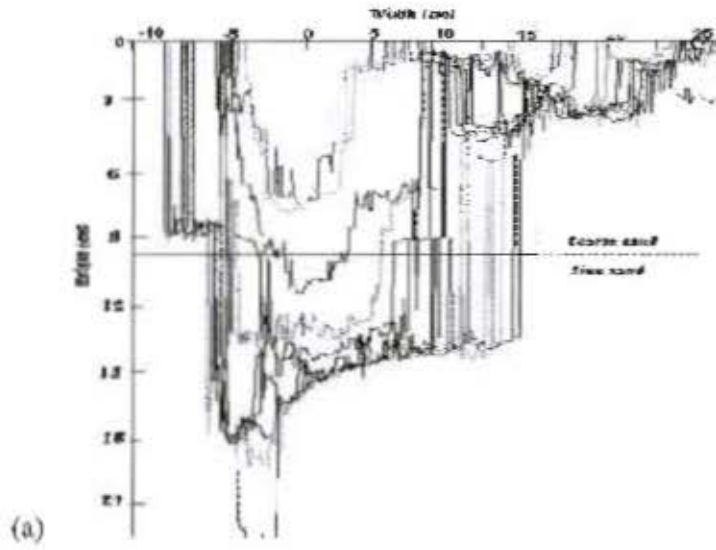
LNAPL Saturation (%)	Volumetric (cm ³ /cm ³)		Average Intensity			
	Coarse sand	Fine Sand	Coarse sand		Fine Sand	
			Soltrol 220	Diesel	Soltrol 220	Diesel
<20%	0	0	214	193,4	157,4	219,5
20 %	8,6	7,4	166	173,3	121	167,2
40 %	17,2	14,8	117	150	77	131,5
60 %	25,8	22,2	76	125	42,4	107
80 %	34,4	29,6	61	102	22,3	60
100 %	43	37	25	80	15	50

According to the calibrated data, it can be assumed that the colour intensity, which expresses LNAPL presence, is a linear function of saturation. Other studies concluded that the hue of the transmitted light is directly related to the water content within the porous media (Kechavarzi et al. 2005).

4. RESULTS AND DISCUSSION

As mentioned above, images of the experimental apparatus were taken at certain time intervals and edited using special MatLab algorithms. Figure 1 shows the LNAPL movement profiles during the spill for the four experiments.

It is evident that the same volume of LNAPL caused a different size and shape of contamination plume in the same unsaturated porous material.



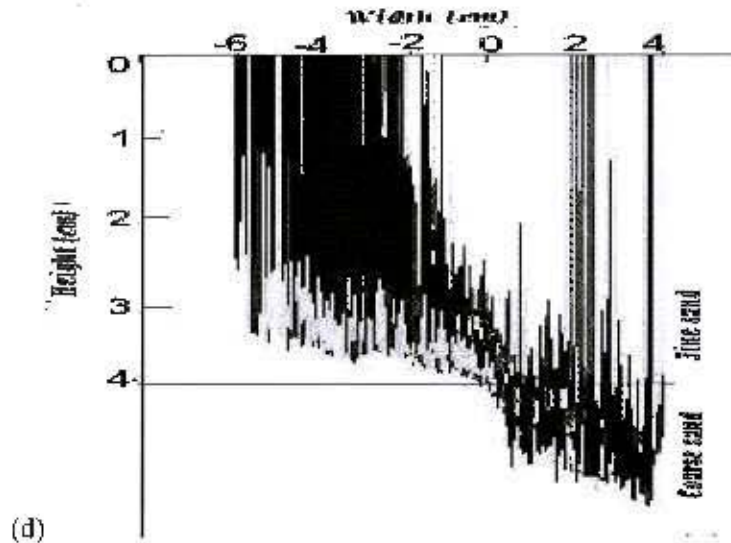


Figure 1. Diesel (a), (b) and Soltrol (c), (d) movement profiles.

According to the results of the image analysis technique, Soltrol flow took place both vertically and horizontally and mainly in the coarse sand layer and less in the fine sand. The migration of the LNAPL was slowed down in the fine layer because of the lower NAPL relative permeability in the fine sand layer (Van Geel et al. 1994). The low unsaturated hydraulic conductivities of a coarse sand prevents large flow rates and as result a semi-permanent retention can be observed, which means that contaminant saturations higher than expected may be retained in layered soils (Walser et al. 1999).

The horizontal movement followed the gravitational one. The maximum horizontal spread of Soltrol was 32 cm for the first experiment and the respective maximum vertical extent was 13 cm within 160 min. According to the image analysis results, saturation equal to 20% and 40% is not often recorded throughout the experiment. Very low and very high saturation was limitedly traced. The dominant saturation percentage was estimated to be between 60%-80% and increased with the depth. The saturation level which was measured in the larger part of the plume area for the first two experiments was about 60%, while 80% saturation was noticed in an area of 683 cm². Also, it was observed that in stratified media higher oil contents are measured at the boundary between less permeable and more permeable layers (Schwille F, 1967).

Diesel fuel distribution during the first experiment also presents different saturation percentages in the plume area. More specifically, although 60% is the average LNAPL saturation, many areas appear to have smaller values of saturation, such as 20% or less, especially during the flow in the fine sand layer. Important changes in Diesel distribution were not observed 270 min after the spill. The maximum depth of Diesel spread was 17 cm below the spill point and 28cm horizontally. The experimental saturation profile shows an effective saturation close to 1 at zero elevation and again at the fine-coarse sand interface (Walser et al. 1999). Comparing the flow of the two LNAPL, it is concluded that Diesel spread is wider and the maximum spread of Soltrol 220 was achieved in a smaller period of time.

During the last two experiments the flow was much more slower, the maximum horizontal spread of LNAPL was 6 cm for the Soltrol experiment and the respective maximum vertical extent was 5,5 cm within 180 min. As far as the second Diesel experiment is concerned the maximum horizontal spread of LNAPL was 8 cm and the maximum vertical extent was 7 cm in

the same period of time. In both experiments with the fine layer of sand being upper the coarse sand layer the saturation was estimated to be low in the fine layer and higher in the coarse sand layer.

In all experiments flow in the fine sand is slower, due to the smaller porosity of the fine sand, compared to the coarse. When redistribution started and gravitational flow became dominant, the rate of horizontal migration, due to capillary forces, became small, compared to the rate of vertical migration, in both experiments. The main difference between the two sets of experiments is that the interface of fine/coarse sand acts as a capillary barrier which prevents strongly the LNAPL to infiltrate in the below fine layer. Whereas, in the interface of coarse/fine sand even though the horizontal movement became dominant the gravitational one also exists. This conclusion is also confirmed by Wilfler et al. who indicate that in case of a wetting fluid imbibing a fine sand overlying a coarse sand, capillary forces will retain the fluid in the fine sand at the interface.

Also, as a result of the image analysis, the following pictures that depict the LNAPL saturation in the soil matrix were created. Figures 2 and 3 show the saturation profiles that correspond to the final images of each experiment.

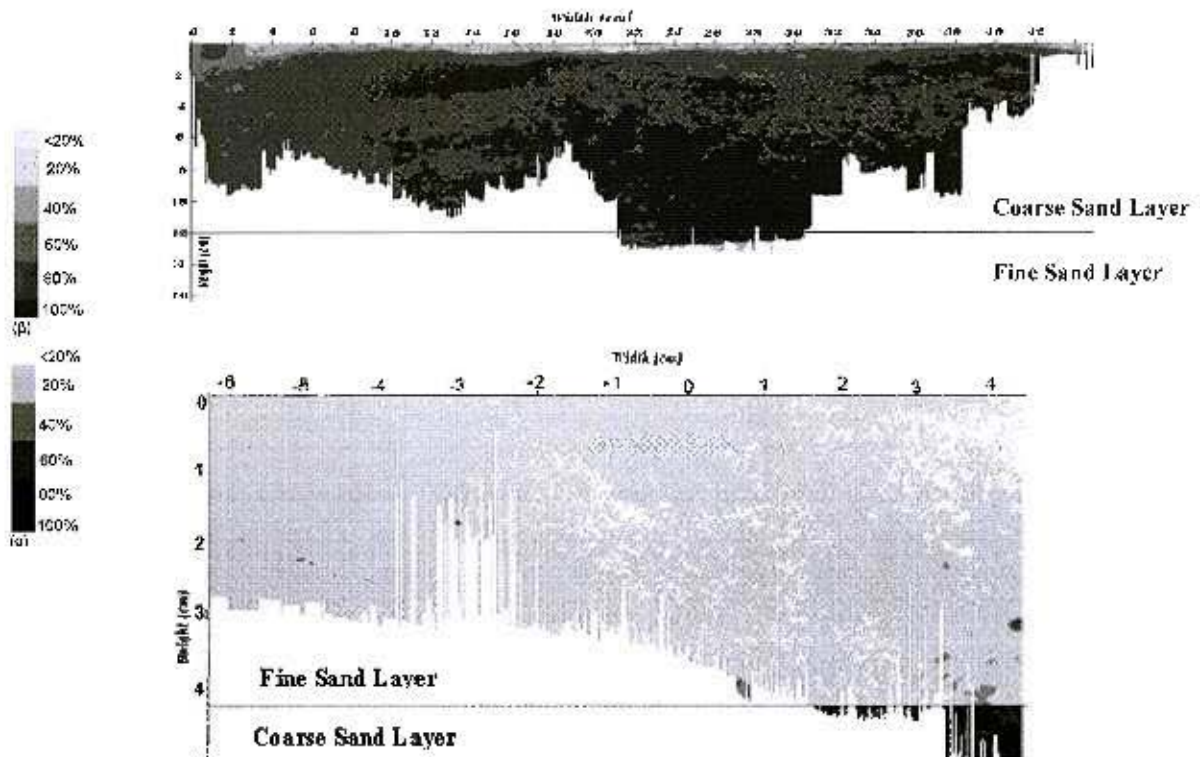


Figure 2. Soltrol final distribution and saturation versus time.

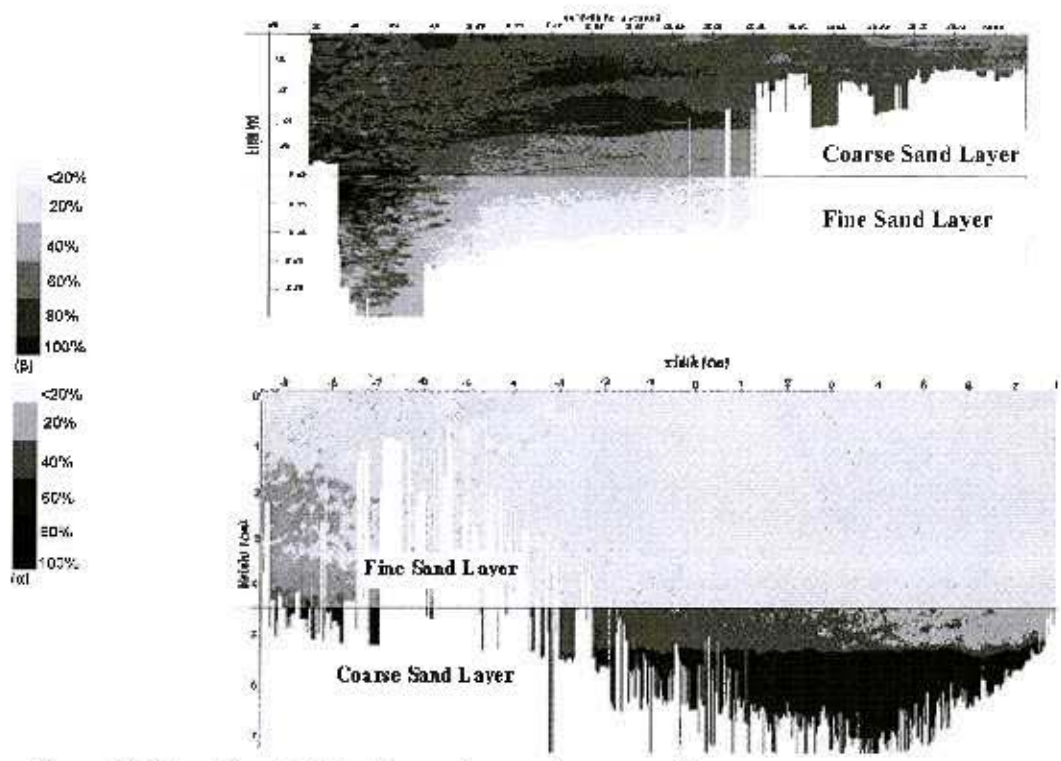


Figure 3. Diesel final distribution and saturation versus time.

Finally, k-s-p curves were created for each one of the experiments. It was concluded that the fine sand had higher capillary pressure due to the pore size.

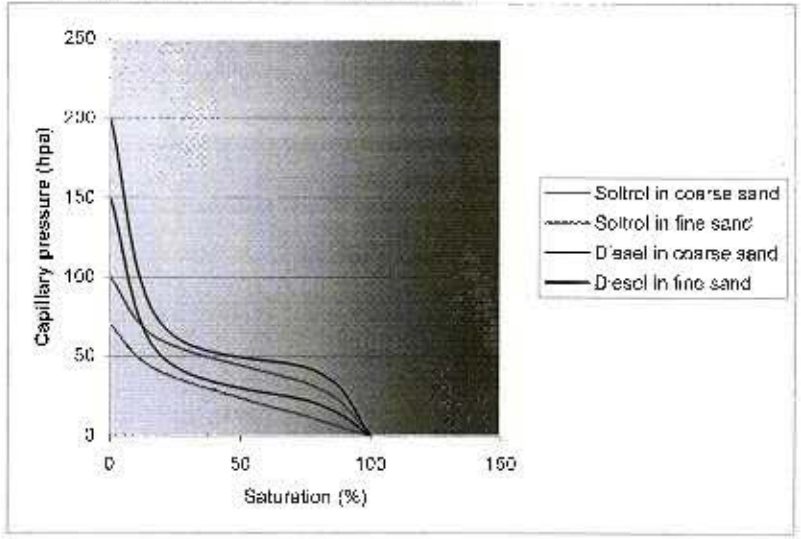


Figure 4. P-S curves for coarse and fine sand and both LNAPL.

5. CONCLUSIONS

Four laboratory experiments were performed to qualitatively study the movement of LNAPL. The image analysis techniques provided a useful non-destructive method of determining the distribution of LNAPL at various time during a spill. Analyzing the flow field in HSI (Hue-Saturation-Intensity) format determined the LNAPL saturation percentage. As it was proved, Soltrol and Diesel Fuel present quite different flow patterns and distribution in the same sand matrix, indicating the difficulty in studying each LNAPL movement and retention in the subsurface in each soil type. Additionally, the sand configuration plays a significant role in the LNAPL retention in layered soils.

Acknowledgments

Authors would like to thank Mr. G. Chrysos, Electronic and Computer Engineer, M.Sc., member of the Microprocessor and Hardware Laboratory, Technical University of Crete, for his valuable help on the MatLab algorithms creation and the image analysis technique application. Also, author M. Aivalioti would like to thank the Public Benefit Foundation "Alexander S. Onassis" for its financial support.

REFERENCES

- Van Geel, P. J., Sykes J. F., (1994) "Laboratory and model simulations of a LNAPL spill in a variably-saturated sand: 1: Laboratory experiment and image analysis Techniques", *Journal of Contaminant Hydrology*, Vol. 17 pp. 1-25.
- E. L. Wipfler, M. Ness, G. D. Broodveld, A. Marsman, S.E.A.T.M. van der Zee, "Infiltration and redistribution of LNAPL into unsaturated layered porous media", *Journal of Contaminant Hydrology*, Vol. 71 pp. 47-66.
- Radhey S. Sharma, Mostafa H.A Mohamed, "An experimental investigation of LNAPL migration in an unsaturated/saturated sand", *Journal of Contaminant Hydrology*, Vol. 70 pp. 305-313.
- Head, K.H. (1992) "Manual of soil laboratory testing", Volume 1, London.
- Kechavarzi C., Soga K. and Illangasekare T.II. (2005) "Two-dimensional laboratory simulation of LNAPL infiltration and redistribution in the vadose zone" *Journal of Contaminant Hydrology*, Vol. 76, pp. 211-233.
- A. Wilson (1988) "What color is color?" *The Electronic System Design Magazine*, pp. 38-44
- Christophe J.G Damault, James A. Throop, David A. DiCarlo Alon Rimmer, Tammo S. Steenhuis, J-Yves Parlange (1997) "Visualization by light transmission of oil and water contents in transient two-phase flow fields", *Journal of Contaminant Hydrology*, Vol. 31 pp. 337-348.
- C. Kechavarzi, K. Soga, P. Wiart, (2000), "Multispectral image analysis method to determine dynamic fluid saturation distribution in two-dimensional three-fluid phase flow laboratory experiments", *Journal of Contaminant Hydrology*, Vol. 46 pp. 265-593.
- Gabriele S. Walser, Tissa H. Illangasekare, Arthur T. Corey (1999) "Retention of liquid contaminants in layered soils", *Journal of Contaminant Hydrology*, Vol. 39 pp. 91-108.
- Schwille F. (1967) *Petroleum contamination of the subsoil-a hydrological problem* In Hepple, P. (ED) *The Joint Problems of the oil and water Industries*. The Institute of Petroleum, London England.